Supporting Information for: Implementation of the Deutsch-Jozsa algorithm in excitonic circuits with quantum dynamics and classical molecular dynamics simulation

Maria A. Castellanos and Adam P. Willard*

Department of Chemistry, Massachusetts Institute of Technology, Cambridge, MA

E-mail: awillard@mit.edu

Contents

S.1 Additional details on the simulation of idealized excitonic circuits in model environments

The population dynamics of all four dyes comprising the idealized circuits in Section 4, for each step in the serial approach are shown in Figure S1. Note that the first step is identical for both versions of the algorithm (*i.e.,* $\hat{\mathcal{H}}_1$), and therefore here the resulting populations are only shown once. On the other hand, the third step population dynamics are shown for both circuits, to illustrate the effect of the different in initial states, even though both circuits evolve with $\hat{\mathcal{H}}_3$. The second step for the constant version is not shown, as the identity oracle operation has no effect on the exciton populations.

S.2 Methodology for the QM/MM simulation of Cyanine excitonic circuits.

S.2.1 All-atom molecular dynamics simulations for Cy3 and Cy5 construct.

The molecular simulations in this paper followed a similar methodology as that described by Hart, *et.al.*[1] Prior to performing the all-atom molecular simulations over the Cy3-Cy5 constructs, a force field was generated for both the Cy3 and Cy5. monomers. The structures for Cy3-oxypropyl and Cy5-oxypropyl were built using the Avogadro software (version 1.2.0),[2] and the geometry was optimized with the restricted Hartree-Fock (RHF) method and the 6-31G(d) basis set, as included in the Q-chem software.[3] The atomic point charges

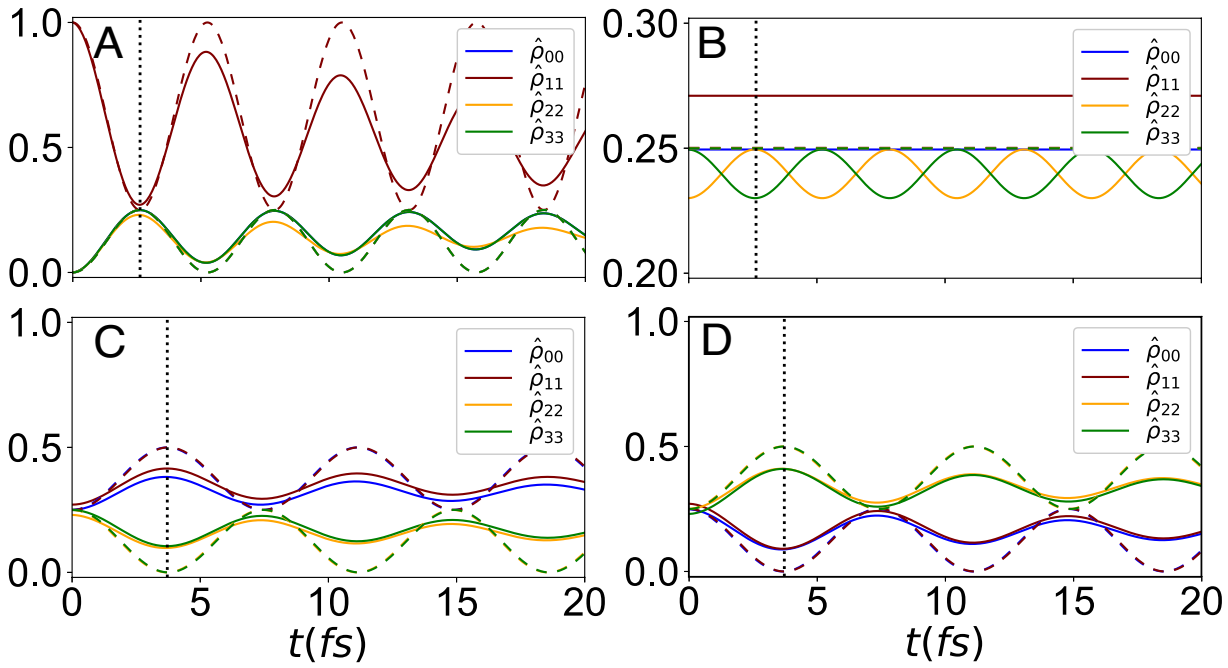

Figure S1: Time-evolution of the populations of the D-J algorithm with a model environment (extension of Figure 2 from the main text). Populations of all four dyes in each excitonic circuit are shown for the (A)first, (B)second and (C)third steps of the balanced version of the D-J algorithm. The third step corresponding to the constant version of the D-J algorithm is depicted in (D).

were generated with a Restrained Electrostatic Potential (RESP) fit also using Q-Chem, and the generalized Amber force field (GAFF)[4] was employed for all force field terms.

The optimized spatial parameters obtained from the genetic algorithm code were used to build the Cy3-Cy5 constructs with the MDAnalysis software,[5,6] using the equilibrium geometries. All-atom Molecular Dynamics (MD) simulations were performed on these cyanine systems using the software Amber18[7] with the GAFF2 force field.[4] The structures were solvated in TIP3P water molecules, and a distance of 10$\mathring{A}$ with respect to the solvent box. Explicit Cl^- ions were added to neutralize the cyanine molecules. Periodic boundary conditions were applied to all MD simulations, and the SHAKE algorithm was applied to constrain the H atoms to their equilibrium bond length. A 12$\mathring{A}$ cutoff was used to calculate the Van der Waals energies, while The Particle Mesh Ewald (PME) method was employed to calculate full electrostatics. The simulations were carried out in a NPT ensemble using the Langevin thermostat for temperature control with a collision frequency of 2 ps^-1, and

the Berendsen barostat for pressure control, with a reference pressure of 1 bar. Prior to the production simulation, a minimization was carried out over the constrained system during 5000 steps. Then, the constrained system was allowed to equilibrate while it was slowly heated to 300 K, for a total time of 10 ps and time-step 1 fs, which was followed by a second equilibration for 5 ps at constant temperature. The production dynamics were then generated at 300 K during a total of 6 ps. A smaller time-step of 0.1 fs was used during this step to carefully simulate the short-time dynamics of interest.

S.2.2 Excited state QM calculations

The geometries for the CY3-CY5 constructs, corresponding to $\hat{\mathcal{H}}_1$ and $\hat{\mathcal{H}}_3$, were sampled from the MD trajectories every 4 fs. For each time frame, the coordinate data for the cyanine molecules was extracted using the MDAnalysis package,[5] and the singlet excited state energies were calculated for each individual molecule using PySCF with the TDDFT 6-31G/B3LYP level of theory.[8]

S.2.3 Comparing different methods to determine excited state transition energies.

In order to find an accurate and inexpensive method to study the fluctuations in the excited state energy gap, ε_{01}, we qualitatively compared the results of employing excited state calculations with different electronic structure methods. We can see, for example, that employing a HF/CIS level of theory leads to larger magnitudes for ε_{01}, compared to a TDDFT approach, and we observe the same behaviour when we increase the accuracy of the DFT functional (*i.e.*, as we go higher in the "Jacob's Ladder"). The effect of changing the basis set in the magnitude of the energy gap is smaller in comparison. However, because the correlation function is independent on the overall magnitude of the energy gap, we are only interested in the relative fluctuations of ε_{01} over time. Except for the HF/CIS and TDDFT B3LYP/STO-6G calculations, we can see that the magnitude of the fluctuations is highly

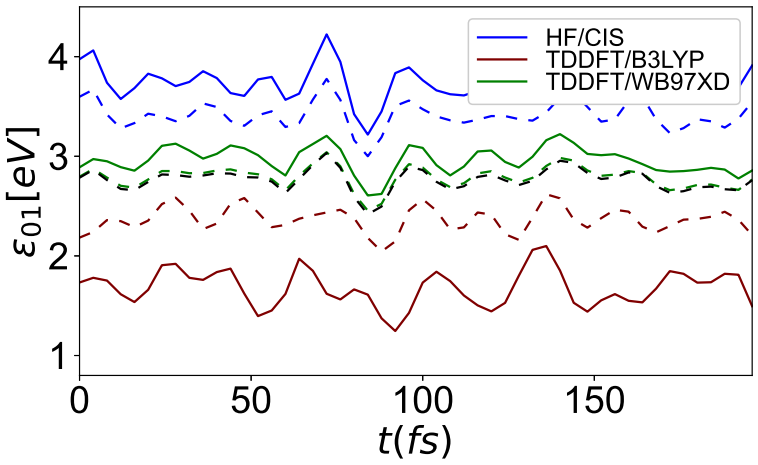

Figure S2: Time evolution of the energy gap between the ground and first excited state, calculated using different levels of theory: HF/CIS and TDDFT, with different combinations of basis sets and density functionals. Here, the solid and dashed lines correspond to calculations employing the STO-6G and 6-31G basis sets, respectively, for the corresponding density functional. The black dashed line corresponds to a TDDFT WB97XD/6-31G(d) level of theory.

similar. In particular, increasing the basis set from WB97XD/6-31G to WB97XD/6-31G(d) has virtually no effect in the time evolution of ε_{01}. Therefore, we choose to employ TDDFT B3LYP/6-31G, as it provides good agreement with a higher level of theory (*e.g,* WB97XD/6-31G(d)), but is still not prohibitively expensive.

S.3 Additional details on the determination of bath fluctuations effect on the Cy3-Cy5 circuits

S.3.1 Fitting the energy-gap correlation function into a functional form.

The parameters employed to fit the correlation function, $C(t)$, into the functional form in Equation 17 are presented in tables S1 to S4, for the $\hat{\mathcal{H}}_1$ excitonic circuit. The resulting fit is compared with the numerically calculated correlation in Figure S3. Note the fit is not exact due to the small number of parameters employed, however, the fit is appropriate to understand the behaviour of the different correlation curves.

Table S1: Fitting parameters for the Cy3(A) dye in the excitonic circuit realizing $\hat{\mathcal{H}}_1$.

Exponential	$a_i[10^{-5}eV]$	$\tau_{c,i}[fs]$	
1	2.000	18.22	
2	0.089	16.88	
Damped	$\tilde{a}_i[10^{-5}eV]$	$\tilde{\tau}_{c,i}[fs]$	$2\pi/\tilde{\omega}_i[fs]$
1	1.000	157.9	21.49
2	4.525	152.7	58.45
3	0.501	1079	20.35
4	5.983	87.60	17.74
5	3.354	41.01	15.84
6	3.875	15.79	12.41

Table S2: Fitting parameters for the Cy5(B) dye in the excitonic circuit realizing $\hat{\mathcal{H}}_1$.

Exponential	$a_i[10^{-5}eV]$	$\tau_{c,i}[fs]$	
1	3.128	19.18	
2	38.71	98.27	
Damped	$\tilde{a}_i[10^{-5}eV]$	$\tilde{\tau}_{c,i}[fs]$	$2\pi/\tilde{\omega}_i[fs]$
1	1.276	117.7	21.60
2	7.805	117.2	82.54
3	1.340	3500	19.98
4	7.253	57.26	16.83
5	10.577	13.27	13.64
6	2.306	1489	17.67

Table S3: Fitting parameters for the Cy3(C) dye in the excitonic circuit realizing $\hat{\mathcal{H}}_1$.

Exponential	$a_i[10^{-5}eV]$	$\tau_{c,i}[fs]$	
1	6.520	0.290	
2	19.10	37.18	
Damped	$\tilde{a}_i[10^{-5}eV]$	$\tilde{\tau}_{c,i}[fs]$	$2\pi/\tilde{\omega}_i[fs]$
1	1.000	1000	20.48
2	0.000	525.2	60.97
3	0.995	2600	22.07
4	8.849	20.00	15.06
5	9.192	71.99	17.81
6	1.065	17800	17.95

Table S4: Fitting parameters for the Cy5(D) dye in the excitonic circuit realizing $\hat{\mathcal{H}}_1$.

Exponential	$a_i[10^{-5}eV]$	$\tau_{c,i}[fs]$	
1	70.00	10.00	
2	70.00	43.33	
Damped	$\tilde{a}_i[10^{-5}eV]$	$\tilde{\tau}_{c,i}[fs]$	$2\pi/\tilde{\omega}_i[fs]$
1	28.24	2000	514.7
2	28.59	2000	171.9
3	3.451	2480	67.99
4	5.755	2392	17.57
5	2.059	2450	27.17
6	4.053	2000	26.31

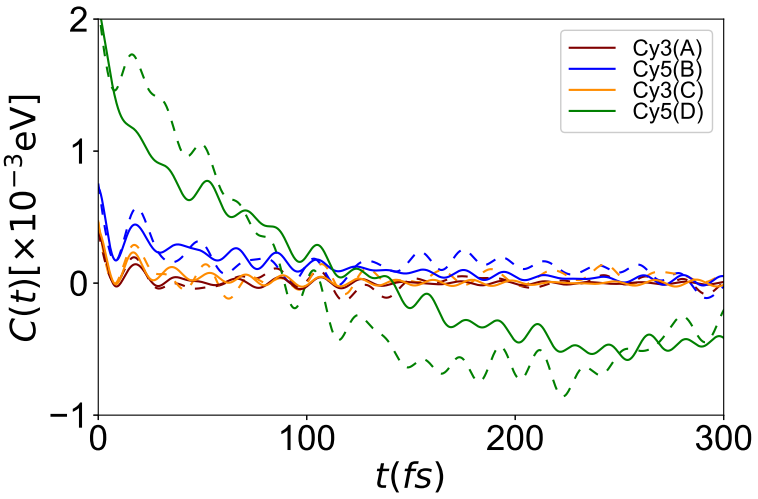

Figure S3: Correlation function for $\hat{\mathcal{H}}_1$ fitted to a double exponential with damped oscillations functional form, as described in the main text. The dashed lines show the time evolution of $C(t)$ as calculated numerically from the data set for ε_{01}.

S.3.2 Analysis of the fluctuations of the torsional angles in the Cyanine circuits.

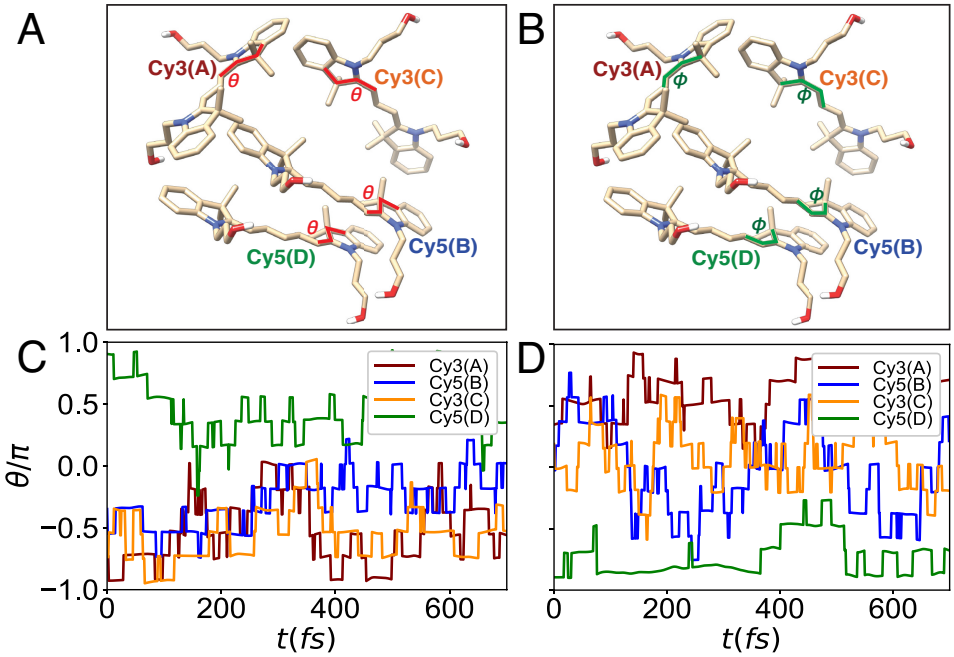

Figure S4: Fluctuations on the relative geometries of the Cyanine molecules for the $\hat{\mathcal{H}}_1$ circuit. The time evolution of two torsional angles is evaluated, θ and ϕ. The angles are indicated in (A) and (B), respectively, while the evolution of these for a space of 700 fs is shown in (C) and (D).

S.3.3 Spectral density via numerical integration of the correlation function.

The spectral density was first calculated through a numerical integration of the correlation function via Equation 16. The resulting noisy spectra is shown in Figure S5 for both circuits studied in this manuscript. The intricate nature of the spectra most likely is due to the lack of sampling data, with $C(t)$ not decaying completely to zero over the time range were $J(\omega)$ was evaluated. However, we can note that, generally, same molecules share the similar peaks, although with varying amplitudes that directly depend on the magnitude of the bath fluctuations for each dye. In particular Cy5(B) in circuit $\hat{\mathcal{H}}_1$ shows a large amplitude frequency mode around 600cm^{-}1. This peak probably corresponds to vibrational mode on the heterocycle ring, and confirms our hypothesis of a comformational change modifying the spectroscopic properties of this dye.

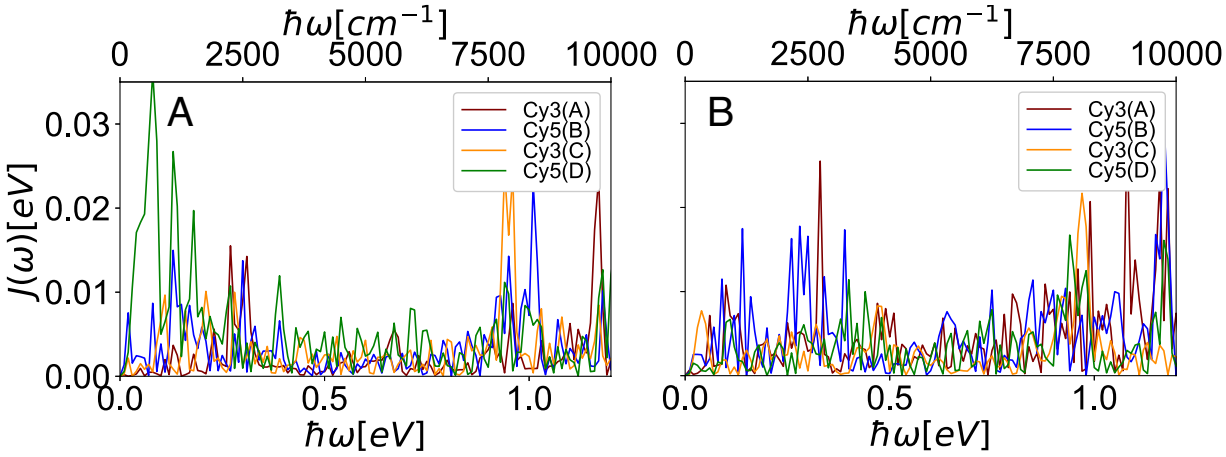

Figure S5: Spectral density, $J(\omega)$ evaluated from the numerical integration of $C(t)$ as in Equation 16, for the circuits evolving as $\hat{\mathcal{H}}_1$ and $\hat{\mathcal{H}}_3$, respectively.

S.3.4 Fitting the numerical spectral density, from a double exponential decaying correlation function.

Assuming the correlation function, $C(t)$, takes a double exponentially decaying functional form we have,

$$C(t) = a_1 e^{-t/\tau_{c,1}} + a_2 e^{-t/\tau_{c,2}}, \tag{S1}$$

which is derived by setting $\tilde{a}_i = 0$ in Equation 17. The corresponding spectral density is derived in the main text (Equation 18), and the numerical spectra in Figure S5 is fitted to this functional form. The fitting parameters are listed in Tables S5 and S6, while the fitted $J(\omega)$ is shown in the main text for both cases.

Table S5: Fitting parameters for the $\hat{\mathcal{H}}_1$ spectral density.

Dye	$a_1[10^{-5}eV]$	$a_2[10^{-5}eV]$	$\tau_{c,1}[fs]$	$\tau_{c,2}[fs]$
Cy3(A)	65.96	65.83	2.513	2.512
Cy5(B)	9581	99.31	2.214	2.215
Cy3(C)	8626	95.71	2.200	2.200
Cy5(D)	140.9	3587	10.00	0.035

Table S6: Fitting parameters for the $\hat{\mathcal{H}}_3$ spectral density.

Dye	$a_1[10^{-5}eV]$	$a_2[10^{-5}eV]$	$\tau_{c,1}[fs]$	$\tau_{c,2}[fs]$
Cy3(A)	159.2	159.2	1.997	1.997
Cy5(B)	185.4	182.8	1.930	1.930
Cy3(C)	125.5	125.5	1.721	1.722
Cy5(D)	154.7	150.3	1.779	1.779

S.3.5 Time-evolution of the populations in the step-by-step constant version of the D-J algorithm with the calculated bath.

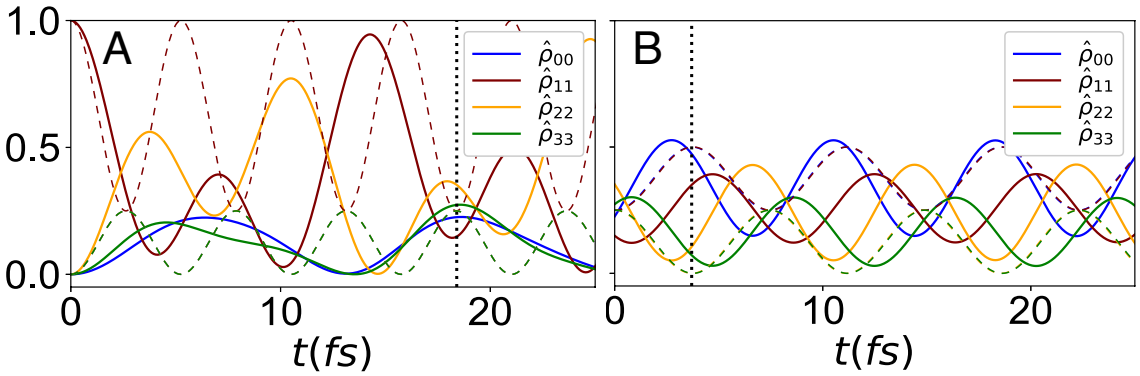

Figure S6: Extension for Figure 7, including the time evolution of all four dyes in the step-by-step D-J algorithm for the first (A), and the third steps (B). The curves corresponding to a perfectly matching spatial arrangement with that described by the Frenkel Hamiltonian, and at closed system conditions, are shown in dashed lines. The corresponding transformation times, $7\tau_1$ and τ_2 are shown in black dotted lines in each plot, as described in the main text.

References

(1) Hart, S. M.; Chen, W. J.; Banal, J. L.; Bricker, W. P.; Dodin, A.; Markova, L.; Vyborna, Y.; Willard, A. P.; Häner, R.; Bathe, M.; Schlau-Cohen, G. S. Engineering couplings for exciton transport using synthetic DNA scaffolds. *Chem* **2021**, *0*.

(2) Avogadro: an open-source molecular builder and visualization tool. Version 1.2.0. `http://avogadro.cc/`.

(3) Shao, Y. et al. Advances in molecular quantum chemistry contained in the Q-Chem 4 program package. *Molecular Physics* **2015**, *113*, 184–215.

(4) Wang, J.; Wolf, R. M.; Caldwell, J. W.; Kollman, P. A.; Case, D. A. Development and testing of a general Amber force field. *Journal of Computational Chemistry* **2004**, *25*, 1157–1174.

(5) Michaud-Agrawal, N.; Denning, E. J.; Woolf, T. B.; Beckstein, O. MDAnalysis: A toolkit for the analysis of molecular dynamics simulations. *Journal of Computational Chemistry* **2011**, *32*, 2319–2327.

(6) Gowers, R.; Linke, M.; Barnoud, J.; Reddy, T.; Melo, M.; Seyler, S.; Domański, J.; Dotson, D.; Buchoux, S.; Kenney, I.; Beckstein, O. MDAnalysis: A Python Package for the Rapid Analysis of Molecular Dynamics Simulations. Proceedings of the 15th Python in Science Conference. 2016; pp 98–105.

(7) Case, D. et al. *AMBER 2018*; University of California, San Francisco, 2018.

(8) Sun, Q.; Berkelbach, T. C.; Blunt, N. S.; Booth, G. H.; Guo, S.; Li, Z.; Liu, J.; McClain, J. D.; Sayfutyarova, E. R.; Sharma, S.; Wouters, S.; Chan, G. K.-L. PySCF: the Python-based simulations of chemistry framework. *WIREs Computational Molecular Science* **2018**, *8*, e1340.